Single-Compartment Neural Models

BENG/BGGN 260 Neurodynamics
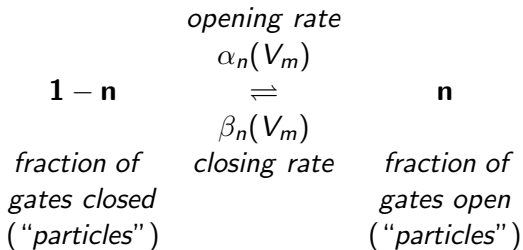
University of California, San Diego

Week 2

Reading Materials

- A.L. Hodgkin and A.F. Huxley, "A Quantitative Description of Membrane Current and Its Application to Conduction and Excitation in Nerve," J. Physiol., vol. 117, pp. 500-544, 1952.

- B. Hille, Ion Channels of Excitable Membranes, Sinauer, 2001, Ch. 2 and 3, pp. 25-92.

- C. Koch, Biophysics of Computation, Oxford Univ. Press, 1999, Ch. 6 through 8, pp. 142-211.

- P. Dayan and L. Abbott, Theoretical Neuroscience, MIT Press, 2001, Ch. 5, pp. 173-177.

- E.M. Izhikevich, Dynamical Systems in Neuroscience, MIT Press, 2007, Ch. 2, pp. 32-49.

- A.F. Strassberg and L.J. DeFelice, "Limitations of the Hodgkin-Huxley formalism: Effects of single channel kinetics on transmembrane voltage dynamics," Neural Computation, vol. 5(6), pp. 843-855, Nov. 1993.
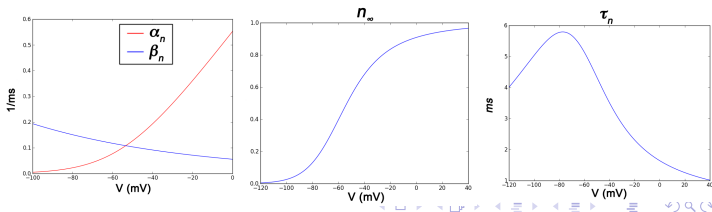
Channel Gate Dynamics

opening rate
$\alpha_n(V_m)$

$\mathbf{1 - n}$ $\rightleftharpoons$ $\mathbf{n}$

$\beta_n(V_m)$

fraction of   *closing rate*   *fraction of*
gates closed   *gates open*
("*particles*")   ("*particles*")

$$\frac{dn}{dt} = \alpha_n(V_m)(1 - n) - \beta_n(V_m)n = \frac{n_\infty(V_m) - n}{\tau_n(V_m)}$$

$$n_\infty = \frac{\alpha_n}{\alpha_n + \beta_n}$$

$$\tau_n = \frac{1}{\alpha_n + \beta_n}$$

Voltage Gated Ion Channels

n: *slow K+ activation;* **m**: *fast Na+ activation;* **h**: *slow Na+ inactivation*
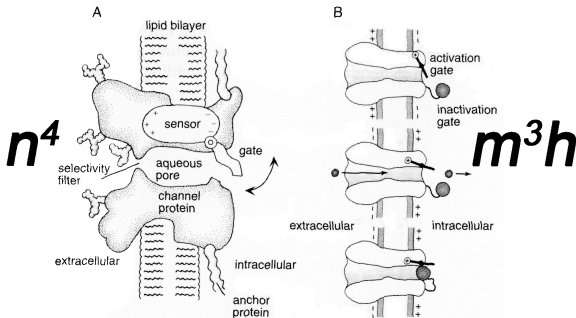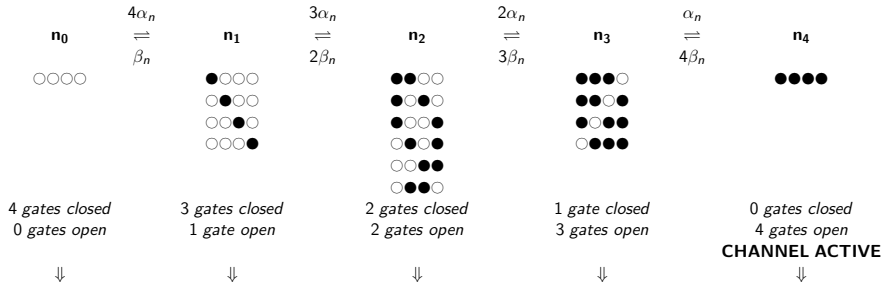

Figure 5.8 Gating of membrane channels. In both figures, the interior of the neuron is to the right of the membrane, and the extracellular medium is to the left. **(A)** A cartoon of gating of a persistent conductance. A gate is opened and closed by a sensor that responds to the membrane potential. The channel also has a region that selectively allows ions of a particular type to pass through the channel, for example, K+ ions for a potassium channel. **(B)** A cartoon of the gating of a transient conductance. The activation gat is coupled to a voltage sensor (denoted by a circled +) and acts like the gate in A. A second gate, denoted by the ball, can block that channel once it is open. The top figure shows the channel in a deactivated (and deinactivated) state. The middle panel shows an activated channel, and the bottom panel shows an inactivated channel. Only the middle panel corresponds to an open, ion-conducting state. (A from Hille, 1992; B from Kandel et al., 1991.)

Dayan & Abbot 2001, pg. 169

K+ Channel Gate Dynamics: 4 - Particle Model

4 "particles" (gates) model: channel active probability $= \mathbf{n_4}$ with:

	$\overset{4\alpha_n}{\underset{\beta_n}{\rightleftharpoons}}$		$\overset{3\alpha_n}{\underset{2\beta_n}{\rightleftharpoons}}$		$\overset{2\alpha_n}{\underset{3\beta_n}{\rightleftharpoons}}$		$\overset{\alpha_n}{\underset{4\beta_n}{\rightleftharpoons}}$	
$\mathbf{n_0}$		$\mathbf{n_1}$		$\mathbf{n_2}$		$\mathbf{n_3}$		$\mathbf{n_4}$
○○○○		●○○○		●●○○		●●●○		●●●●
		○●○○		●○●○		●●○●		
		○○●○		●○○●		●○●●		
		○○○●		○●●○		○●●●		
				○○●●				
				○●●○				
4 gates closed		3 gates closed		2 gates closed		1 gate closed		0 gates closed
0 gates open		1 gate open		2 gates open		3 gates open		4 gates open
								CHANNEL ACTIVE

$$n_0 + n_1 + n_2 + n_3 + n_4 = 1, \; and :$$

$$
\begin{aligned}
\frac{dn_0}{dt} &= -4\alpha_n n_0 & +\beta_n n_1 \\
\frac{dn_1}{dt} &= 4\alpha_n n_0 & -(3\alpha_n + \beta_n)\, n_1 & +2\beta_n n_2 \\
\frac{dn_2}{dt} &= 3\alpha_n n_1 & -(2\alpha_n + 2\beta_n)\, n_2 & +3\beta_n n_3 \\
\frac{dn_3}{dt} &= 2\alpha_n n_2 & -(\alpha_n + 3\beta_n)\, n_3 & +4\beta_n n_4 \\
\frac{dn_4}{dt} &= \alpha_n n_3 & -4\beta_n n_4
\end{aligned}
$$

K+ Channel Gate Dynamics: Reduced Model

| n_0 | $\overset{4\alpha_n}{\underset{\beta_n}{\rightleftharpoons}}$ | n_1 | $\overset{3\alpha_n}{\underset{2\beta_n}{\rightleftharpoons}}$ | n_2 | $\overset{2\alpha_n}{\underset{3\beta_n}{\rightleftharpoons}}$ | n_3 | $\overset{\alpha_n}{\underset{4\beta_n}{\rightleftharpoons}}$ | n_4 |

4 gates closed   3 gates closed   2 gates closed   1 gate closed   0 gates closed
0 gates open   1 gate open   2 gates open   3 gates open   4 gates open
                                                                       CHANNEL ACTIVE

$\Downarrow$ $\Downarrow$ $\Downarrow$ $\Downarrow$ $\Downarrow$

-Reduced (equivalent) model: channel active probability = n^4 with:

$\Downarrow$ $\Downarrow$ $\Downarrow$ $\Downarrow$ $\Downarrow$

$$n_0 = (1-n)^4 \qquad n_1 = 4n(1-n)^3 \qquad n_2 = 6n^2(1-n)^2 \qquad n_3 = 4n^3(1-n) \qquad n_4 = n^4$$

$$\left[\begin{array}{c} \overset{\alpha_n}{1-n \;\; \rightleftharpoons \;\; n} \\ \underset{\beta_n}{\circ \qquad \bullet} \end{array} \right]^4$$

$$\underbrace{\qquad\qquad\qquad\qquad}$$

$$\frac{dn}{dt} = \alpha_n(1-n) - \beta_n n$$

Na+ Channel Gate Dynamics: 4 - Particle Model

-4 "particles" (gates) model: channel active probability = s_{31}

CHANNEL ACTIVE

$$s_{01} = (1-m)^3 h \qquad s_{11} = 3m(1-m)^2 h \qquad s_{21} = 3m^2(1-m)h \qquad s_{31} = m^3 h$$

all gates open/
non − inactivated

○○○▲	●○○▲	●●○▲	●●●▲
	○●○▲	●○●▲	
	○○●▲	○●●▲	

$$
\begin{array}{cccccccc}
\mathbf{s_{01}} & \overset{3\alpha_m}{\underset{\beta_m}{\rightleftharpoons}} & \mathbf{s_{11}} & \overset{2\alpha_m}{\underset{2\beta_m}{\rightleftharpoons}} & \mathbf{s_{21}} & \overset{\alpha_m}{\underset{3\beta_m}{\rightleftharpoons}} & \mathbf{s_{31}}
\end{array}
$$

$\alpha_h \uparrow\downarrow \beta_h$ $\qquad\qquad$ $\alpha_h \uparrow\downarrow \beta_h$ $\qquad\qquad$ $\alpha_h \uparrow\downarrow \beta_h$ $\qquad\qquad$ $\alpha_h \uparrow\downarrow \beta_h$

$$
\begin{array}{cccccccc}
\mathbf{s_{00}} & \overset{3\alpha_m}{\underset{\beta_m}{\rightleftharpoons}} & \mathbf{s_{10}} & \overset{2\alpha_m}{\underset{2\beta_m}{\rightleftharpoons}} & \mathbf{s_{20}} & \overset{\alpha_m}{\underset{3\beta_m}{\rightleftharpoons}} & \mathbf{s_{30}}
\end{array}
$$

○○○△	●○○△	●●○△	●●●△
	○●○△	●○●△	
	○○●△	○●●△	

$$s_{00} = (1-m)^3(1-h) \qquad s_{10} = 3m(1-m)^2(1-h) \qquad s_{20} = 3m^2(1-m)(1-h) \qquad s_{30} = m^3(1-h)$$

Koch, Ch. 8.2, pg. 200-202

Na+ Channel Gate Dynamics: Reduced Model

CHANNEL ACTIVE

$s_{01} = (1-m)^3 h$ $s_{11} = 3m(1-m)^2 h$ $s_{21} = 3m^2(1-m)h$ $s_{31} = m^3 h$

all gates open/
non − inactivated

○○○▲   ●○○▲ / ○●○▲ / ○○●▲   ●●○▲ / ●○●▲ / ○●●▲   ●●●▲

$$\mathbf{s_{01}} \quad \overset{3\alpha_m}{\underset{\beta_m}{\rightleftharpoons}} \quad \mathbf{s_{11}} \quad \overset{2\alpha_m}{\underset{2\beta_m}{\rightleftharpoons}} \quad \mathbf{s_{21}} \quad \overset{\alpha_m}{\underset{3\beta_m}{\rightleftharpoons}} \quad \mathbf{s_{31}}$$

$\alpha_h \uparrow\downarrow \beta_h$ $\alpha_h \uparrow\downarrow \beta_h$ $\alpha_h \uparrow\downarrow \beta_h$ $\alpha_h \uparrow\downarrow \beta_h$

$$\mathbf{s_{00}} \quad \overset{3\alpha_m}{\underset{\beta_m}{\rightleftharpoons}} \quad \mathbf{s_{10}} \quad \overset{2\alpha_m}{\underset{2\beta_m}{\rightleftharpoons}} \quad \mathbf{s_{20}} \quad \overset{\alpha_m}{\underset{3\beta_m}{\rightleftharpoons}} \quad \mathbf{s_{30}}$$

○○○△   ●○○△ / ○●○△ / ○○●△   ●●○△ / ●○●△ / ○●●△   ●●●△

$s_{00} = (1-m)^3(1-h)$ $s_{10} = 3m(1-m)^2(1-h)$ $s_{20} = 3m^2(1-m)(1-h)$ $s_{30} = m^3(1-h)$

⇓   ⇓   ⇓   ⇓
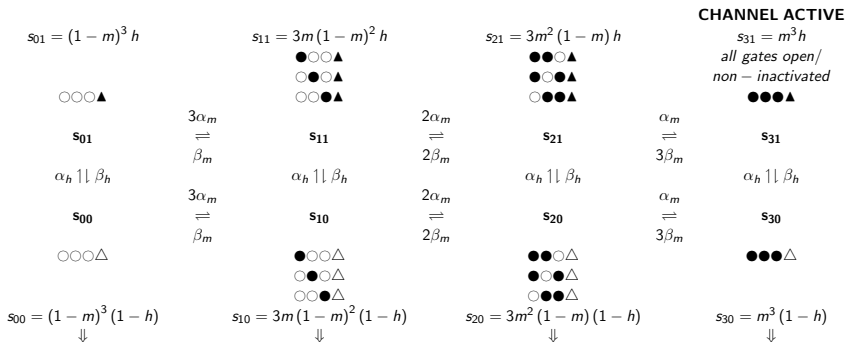
-Reduced (equivalent) model: channel active probability = $m^3 h$ with:

FAST ACTIVATION   *SLOW INACTIVATION*

$$\begin{bmatrix} & \alpha_m & \\ \mathbf{1-m} & \rightleftharpoons & \mathbf{m} \\ \circ & \beta_m & \bullet \\ & & open \end{bmatrix}^3 \begin{bmatrix} & \alpha_h & \\ \mathbf{1-h} & \rightleftharpoons & \mathbf{h} \\ \triangle & \beta_h & \blacktriangle \\ & & non-inactivated \end{bmatrix} \begin{cases} \frac{dm}{dt} = \alpha_m(1-m) - \beta_m m \\ \frac{dh}{dt} = \alpha_h(1-h) - \beta_h h \end{cases}$$
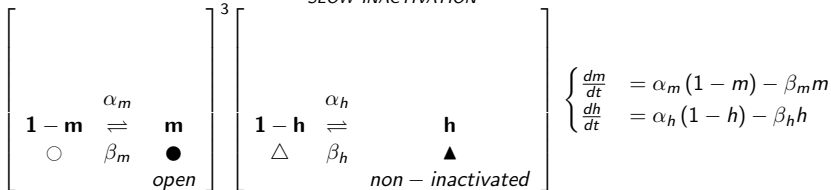
HH Activation and Inactivation Functions

n: *slow K+ activation*
m: *fast Na+ activation*
h: *slow Na+ inactivation*
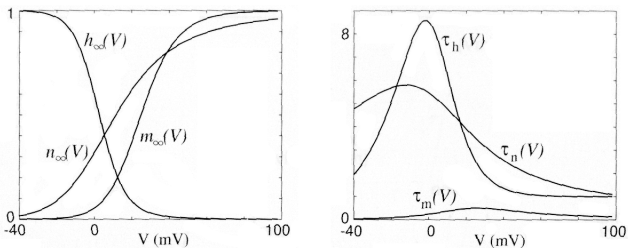
Figure 2.13

Steady-state (in)activation functions (left) and voltage-dependent time constants (right) in the Hodgkin-Huxley model.

Izhikevich 2007, pg. 39

$$m^3 h \, \overline{g}_{Na}$$

$$n^4 \, \overline{g}_K$$
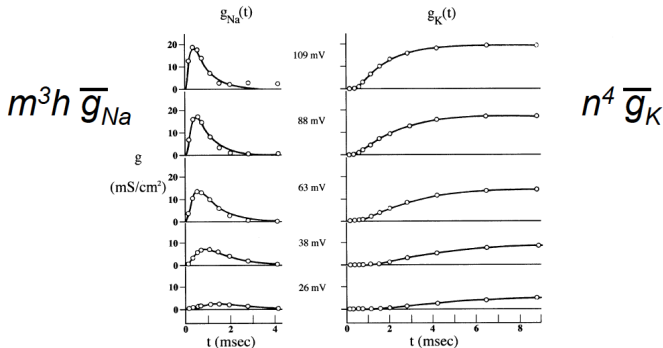
Fig. 6.4 K+ and Na+ Conductances During a Voltage Step

Experimentally recorded (circles) and theoretically calculated (smooth curves) changes in G_{Na} and G_K in the squid giant axon at $6.3°$ C during depolarizing voltage steps away from the resting potential (which here, as throughout this chapter, is set to zero). For large voltage changes, G_{Na} briefly increases before it decays back to zero (due to *inactivation*), while G_K remains activated. Reprinted by permission from Hodgkin (1958).

n: *slow K+ activation*; **m**: *fast Na+ activation*; **h**: *slow Na+ inactivation*

Koch 1999, pg. 149

Hodgkin-Huxley Model *

Squid axon:

$$C_m \frac{dV_m}{dt} = I_{ext} \; \underbrace{- \bar{g}_K n^4 (V_m - E_K)}_{I_K} \; \underbrace{- \bar{g}_{Na} m^3 h (V_m - E_{Na})}_{I_{Na}} \; \underbrace{- g_L (V_m - E_L)}_{I_L}$$

$C_m = 1 \mu F/cm^2$

$E_K = -12 \, mV$ $E_{Na} = 120 \, mV$ $E_L = 10.6 \, mV$

$\bar{g}_K = 36 \, mS/cm^2$ $\bar{g}_{Na} = 120 \, mS/cm^2$ $g_L = 0.3 \, mS/cm^2$

$(mS = \mu A/mV)$

$$\frac{dn}{dt} = \alpha_n (1-n) - \beta_n n = \frac{n_\infty - n}{\tau_n}; \quad \alpha_n (V_m) = \frac{10 - V_m}{100(e^{1-V_m/10}-1)}; \quad \beta_n (V_m) = \frac{1}{8} e^{-V_m/80}$$

$$\frac{dm}{dt} = \alpha_m (1-m) - \beta_m m = \frac{m_\infty - m}{\tau_m}; \quad \alpha_m (V_m) = \frac{25 - V_m}{100(e^{2.5-V_m/10}-1)}; \quad \beta_m (V_m) = 4 e^{-V_m/18}$$

$$\frac{dh}{dt} = \alpha_h (1-h) - \beta_h h = \frac{h_\infty - h}{\tau_h}; \quad \alpha_h (V_m) = \frac{7}{100} e^{-V_m/20}; \quad \beta_h (V_m) = \frac{1}{1+e^{3-V_m/10}}$$

α_x and β_x in units $1/ms$; V_m in units mV

* V_m slightly shifted by $65 mV$ so that $E_{rest} \equiv 0 mV$

Hodgkin-Huxley Dynamics
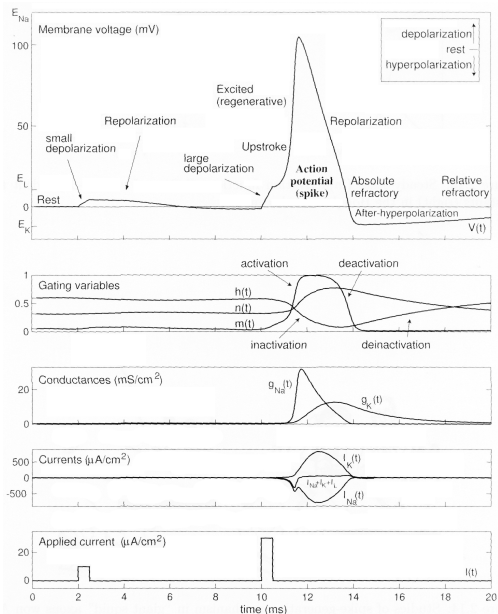
Figure 2.15

Action potential in the Hodgkin-Huxley model.

Izhikevich 2007, pg. 40

From Hodgkin-Huxley to FitzHugh-Nagumo

Fig. 7.1 Reducing the Hodgkin-Huxley Model to the FitzHugh-Nagumo System

Evolution of the space-clamped Hodgkin-Huxley and the FitzHugh-Nagumo equations in response to a current step of amplitude 0.18 nA in A and B and of amplitude I=0.35 in C and D. **(A)** Membrane potential $V(t)$ and sodium activation $m(t)$ (see also Fig. 6.8). Sodium activation closely follows the dynamics of the membrane potential. **(B)** Sodium inactivation 1-h and potassium activation n of the Hodgkin-Huxley system. **(C)** "Excitability" $V(t)$ of the two-dimensional FitzHugh-Nagumo equations (Eqs. 7.1) with constant parameters has a very similar time course to V and m of the squid axon (notice the different scaling). **(D)**The "accommodation" variable W shows modulations similar to $1 - h$ and n of the Hodgkin-Huxley equations.

Koch 1999, pg. 174
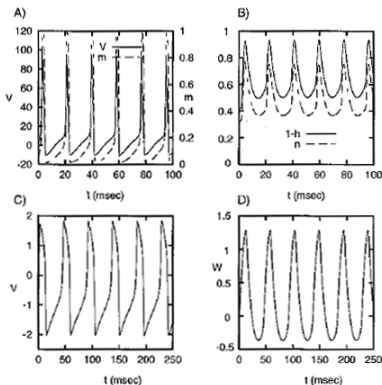
FitzHugh-Nagumo Model

Simplification of Hodgkin-Huxley, reduced to 2 dimensions:

Excitability : $\frac{d}{dt}V = V - \frac{V^3}{3} - W + I_{ext}.$

models fast dynamics of V_m and m activation

Accommodation : $\frac{d}{dt}W = \phi(V + \alpha - \beta W)$

models slow dynamics of n and $1 - h$ inactivation

$\phi = 0.08 \quad \alpha = 0.7 \quad \beta = 0.8$

Facilitates theoretical analysis of stability & dynamics, at the expense of accuracy.

Morris-Lecar Model

Barnacle muscle fibers:

$$C_m \frac{dV_m}{dt} = I_{ext} \underbrace{- \bar{g}_K w \left(V_m - E_K\right)}_{I_K} \underbrace{- \bar{g}_{Ca} m_\infty \left(V_m - E_{Ca}\right)}_{I_{Ca}} \underbrace{- g_L \left(V_m - E_{rest}\right)}_{I_L}$$

$$C_m = 1\mu F/cm^2 \qquad E_K = -70\,mV \qquad E_{Ca} = 100\,mV \qquad E_{rest} = -50\,mV$$

$$\bar{g}_K = 2.0\,mS/cm^2 \qquad \bar{g}_{Ca} = 1.1\,mS/cm^2 \qquad g_L = 0.5\,mS/cm^2$$

$$\tau_w \left(V_m\right) \frac{dw}{dt} = w_\infty \left(V_m\right) - w; \qquad w_\infty \left(V_m\right) = \tfrac{1}{2}\left(1 + tanh\tfrac{V_m}{30}\right); \quad \tau_w \left(V_m\right) = \frac{5}{cosh\frac{V_m}{60}}\,[units\;ms]$$

$$m_\infty \left(V_m\right) = \tfrac{1}{2}\left(1 + tanh\tfrac{V_m+1}{15}\right)$$

The simplifying assumption $\tau_m \ll \tau_w$ leads to a 2-D dynamical model, like Fitzhugh-Nagumo.

Individual Channels and Stochastic Conductance

A) Unitary Sodium Currents

B) Ensemble Average

$m^3 h \, \overline{g}_{Na}$
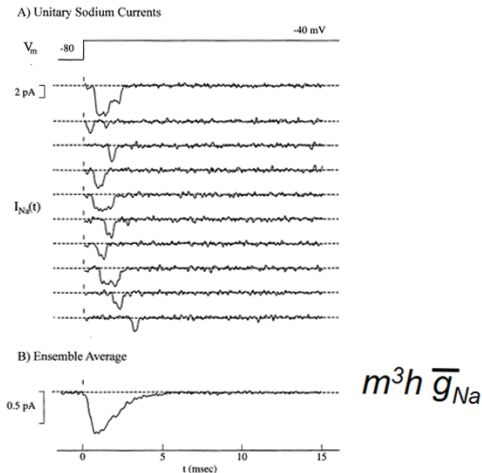
Fig. 8.6 Stochastic Openings of Individual Sodium Channels

(A) Random opening and closing of a handful of fast sodium channels in a mouse muscle cell. The membrane potential was stepped from -80 to -40 mV; the first trial reveals the simultaneous opening of two Na+ channels, while on all other trials, only a single channel was open. **(B)** Averaging over 352 such trials leads to a smoothly varying current in accordance with the $m^3 h$ model of Hodgkin and Huxley. Experiment carried out at $15°$ C. Reprinted by permission from Patlak and Ortiz (1986).

Koch 1999, pg. 203.

Individual Channels and Stochastic Conductance

Fig. 8.7 Simulated Life History of Individual Sodium Channels

The membrane potential in a simulated membrane patch containing a variable number of Na+ channels was stepped from $V_0 = 0$ to $V_1 = 50$ mV at 5 msec (arrow). The normalized conductance associated with the eight-state Markov model shown in Fig. 8.5 was evaluated numerically for several trial runs (see Strassberg and DeFelice, 1993). As the number of channels is increased from 6 to 600, the graded and deterministic nature of the (normalized) sodium conductance emerges from the binary and stochastic single-channel behavior. The top trace shows the conductance computed using the continuous time-course (approximating $\left(1 - e^{-t/\tau_m}\right)^3 e^{-t/\tau_h}$) formalism of Hodgkin and Huxley (1952). This figure should be compared against the experimentally recorded sodium current through a few channels in Fig. 8.6B. Reprinted in modified form by permission from Strassberg and DeFelice (1993).

$m^3 h \, \overline{g}_{Na}$
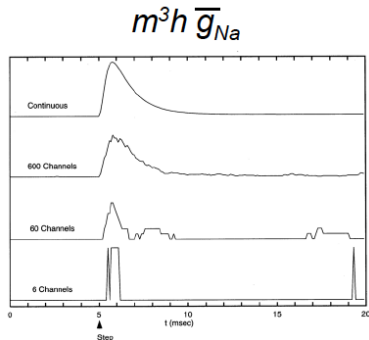
Koch 1999, pg. 206.

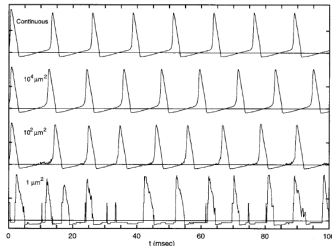# Individual Channels and Action Potentials

Fig. 8.8 Action Potentials and Single Channels

Computed membrane potential (relative to V_{rest} indicated by horizontal lines) in different size patches of squid axon membrane populated by a constant density of Na+ and K+ channels. The space-clamped membrane is responding to a current injection of 100 $pA/\mu m^2$. The transitions of each all-or-none channel are described by its own probabilistic Markov model (the eight-state model in Fig. 8.5 for the Na+ channel and the simplest possible five-state linear model for the K+ channel). For patches containing dozens or fewer channels it becomes impossible to define action potentials unambiguously, since the opening of one or two channels can rapidly depolarize the membrane (not shown). As the membrane potential acts on 1000 or more binary and stochastic channels, the response becomes quite predictable, and merges int the behavior expected by a numberical integration of the Hodgkin-Huxley equations for continuous and deterministic currents (top trace). The density is set to 60 Na+ channels and 18 K+ channels per square micrometer, each with a single channel conductance γ of 20 pS. All other values are as specified in the standard Hodgkin-Huxley model. Reprinted in modified form by permission from Strassberg and DeFelice (1993).

-Shot noise in action potentials due to stochastic individual channels
-Spontaneous, Poisson distributed action potentials even without input (Fig. 8.9, pg. 208)

Koch 1999, pg. 207